Available online at www.sciencedirect.com
ScienceDirect
Earth and Planetary Science Letters 254 (2007) 239–255
EPSL
www.elsevier.com/locate/epsl

Impact of riser reconstructions on estimation of secular variation in rates of strike–slip faulting: Revisiting the Cherchen River site along the Altyn Tagh Fault, NW China

Eric Cowgill *

Department of Geology, University of California, Davis, CA 95616, United States

Received 13 June 2006; received in revised form 4 September 2006; accepted 4 September 2006
Available online 12 January 2007
Editor: M.L. Delaney

Abstract

Slip rates are heavily contested for many of the first-order strike–slip faults within the Indo–Asian collision zone. Rates determined geodetically are generally lower than those reported using reconstructions of offset landforms, and it is unclear if this discrepancy reflects true secular variation in slip history, systematic errors in interpretation, or both. Here I examine the methods used to derive slip rates from reconstructions of displaced fluvial risers, and show that such rates are subject to potentially important uncertainties that have largely been overlooked. Review of published data demonstrates that the slip rate can vary by a factor of 1.2 to 5 for the same site, depending on whether the reconstruction uses the age of the upper or lower terrace for the initiation of riser offset. To reduce this epistemic uncertainty, I have developed six geomorphic indices that can be used to identify the most accurate end-member reconstruction: (1) comparison of riser offset with inset channel width; (2) similarity of riser and tread displacements; (3) morphological analysis of the scarp profile; (4) riser deflection in plan view; (5) diachroneity of terrace abandonment; and (6) whether riser crests or bases yield the slip vector. Without the use of these geomorphic observations the epistemic uncertainty associated with current methods for determining slip rate from offset fluvial risers is likely to be so large that there is no resolvable discrepancy between the GPS and geologic rates within the Indo–Asian collision zone. Application of three of these indices to new field mapping of the Cherchen He (River) Site (~86.4°E) along the central Altyn Tagh Fault yields a revised slip rate of 9.4±2.3 mm/yr, equivalent within error to the rates previously derived from GPS and paleoseismic studies. Although reinterpretation of published data from the Sulamu Tagh site (~87.4°) is consistent with this revised rate, additional work is needed to reconcile this result with some of the rates reported near Aksay (~94°E).

Keywords: fluvial terrace riser; secular variation in slip rate; active strike–slip faulting; Altyn Tagh Fault; Cherchen He

1. Introduction

The Indo–Asian collision provides an excellent opportunity to link intracontinental deformation with far-field plate motions and thereby move from a purely kinematic picture of this archetypal continental collision to an understanding of its dynamics. The orogen is cut by several major strike–slip faults, and although establishing accurate Quaternary slip rates for these >1000 km-long structures is critical for understanding the orogen, such rates are generally disputed. For example, two apparently

* Tel.: +1 530 754 6574; fax: +1 530 752 0951.
E-mail address: cowgill@geology.ucdavis.edu.

0012-821X/$ - see front matter © 2006 Elsevier B.V. All rights reserved.
doi:10.1016/j.epsl.2006.09.015

contradictory rates have been reported for the active, left-slip Altyn Tagh Fault, which locally defines the northwestern margin of Tibet. While both GPS [1–5] and paleoseismic studies [6–8] have yielded slip rates of ~10 mm/yr, reconstructions of displaced landforms yield rates almost three times faster, ~27 mm/yr (e.g., [9]). Disparate rates have also been reported for the active, right-slip Karakoram Fault, where offset Holocene (1–14 ka) features indicate a rate of 4±1 mm/yr [10], but reconstruction of Pleistocene (20–140 ka) features yields a rate of 10.7±0.7 mm/yr [11].

In both cases it remains unclear if the discrepant data reflect true secular variation in slip rate [9,11,12] or errors in how the rates were determined [13–15]. Resolving this dispute is important. If these faults show secular variation, then determining their slip histories will yield much-needed observational data to test mechanical models seeking to explain this behavior (e.g., [16–18]). Important insights can be obtained by determining both the amplitude and frequency of the temporal variations in slip rate (e.g., [19]) and the extent to which slip histories on separate faults are correlated or anti-correlated over time [20–23]. Determining accurate slip rates is also important for testing divergent kinematic models of Asian deformation (e.g., [15]), and in particular, for determining whether such deformation is more plate-like (e.g., [24,25]) or non-plate-like (e.g., [26,27]).

Determining a rate of strike–slip faulting is simple in principle because only two measurements are needed: a magnitude of offset and the time over which this displacement accrued. Fluvial terrace risers are erosional escarpments that separate two stream terraces of different age and elevation (Fig. 1), and commonly provide

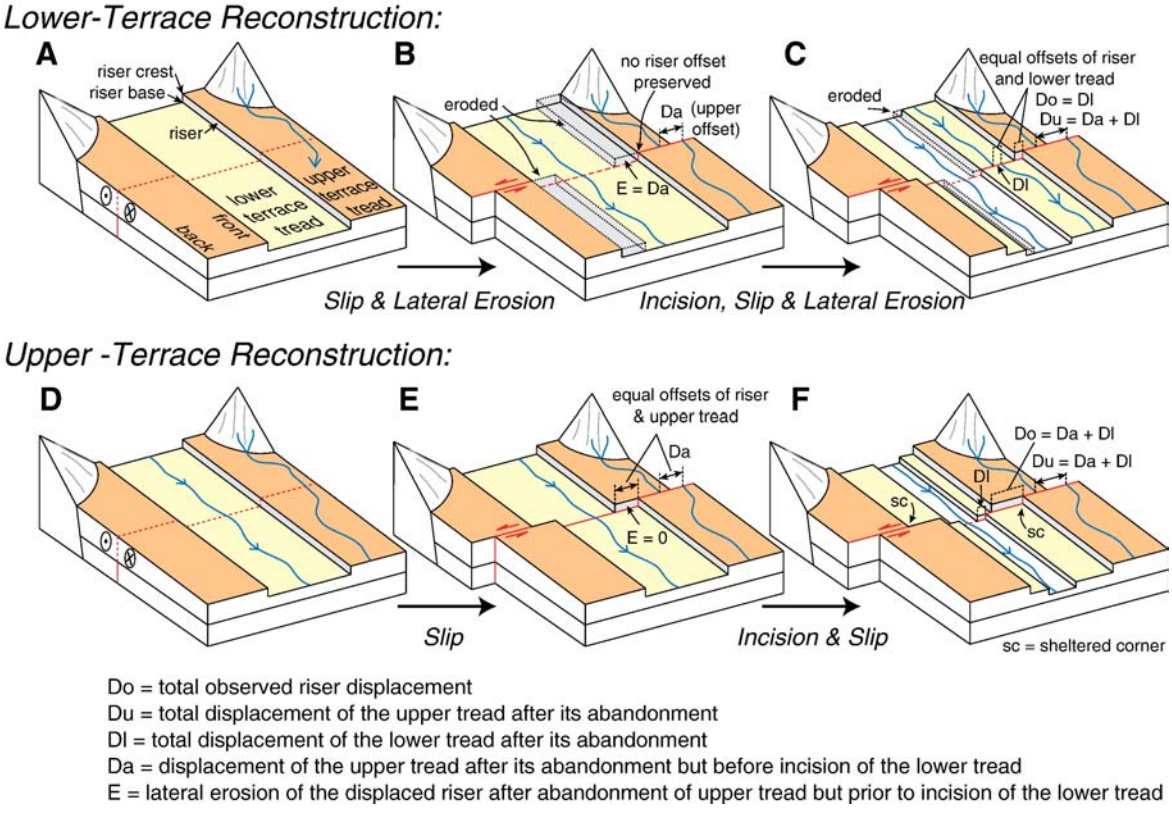

Fig. 1. Block diagrams showing terrace nomenclature and two end-member models for linking riser offsets with terrace abandonment ages to determine rates of strike–slip faulting. Lower- and upper-terrace reconstructions are shown in panels (A–C) and (D–F), respectively. (A) Initial configuration, showing stream after incision of upper tread but before displacement of lower terrace. Blue line on upper tread is a primary feature that tracks total offset of upper tread (Du). (B) Lower-terrace model presumes all riser offset is removed by lateral erosion ($E=D_a$) as long as stream occupies lower tread. As a result, stream channel must widen by at least D_a. At this stage $D_u=D_a$ and $D_o=0$. Gray boxes denote eroded material. (C) After incision of the lower tread, observed riser offset is equivalent to magnitude of slip that postdates lower tread incision ($D_o=D_l$). Total offset of upper tread is larger than D_o and is given by $D_u=D_a+D_l$. (D) Same as (A). (E) Upper-terrace model assumes no lateral erosion of riser ($E=0$). Thus riser offset and upper tread displacement (D_a) are equal. (F) Riser continues to accumulate slip after incision of lower tread such that $D_o=D_u=D_a+D_l$. Originally drafted by Ryan Gold after figures in Van der Woerd et al. [28] and Mériaux et al. [12].

excellent piercing lines for determining displacement because they are typically linear, sharply defined features, the age of which is bracketed by the ages of the flanking terraces. Numerous workers have derived slip rates from offset fluvial risers in Asia [9,28–31] and elsewhere [32–35]. Because of the simplicity in measuring these displaced markers and the relative complexity of establishing the age of the flanking terraces, analysis of slip-rate data is typically weighted towards the interpretation of the age data.

In contrast to the well-recognized concerns regarding dating landforms (e.g., [10–12,14,36,37]), potentially critical ambiguities regarding the geomorphic/structural reconstruction of such landforms have largely been overlooked (e.g., Fig. 1). In particular, little attention has been paid to determining which terrace age most accurately dates initiation of riser displacement, although Mériaux et al. [12] recently discussed this question, and several studies have suggested that this ambiguity provides a solution to discrepant GPS and geological slip rates [13,15]. It is generally difficult to directly date an offset riser, although recent work shows considerable promise in overcoming this problem [38]. As a result, the abandonment age of one of the terraces flanking the riser is typically used as a proxy for the initiation of offset. But to what extent does such an age truly correspond to the observed riser offset, and should the terrace at the bottom of the riser or the one at the top be used? Due to this ambiguity, slip rates derived by combining riser offsets with terrace ages depend on an integrated geomorphic and structural reconstruction of the site. Errors in the assumed reconstruction will thus propagate into errors in the slip rate (e.g., [12,31,39,40]).

This paper has two goals. I first illustrate how errors in the geomorphic reconstruction of an offset fluvial riser will bias slip rates, and in this way, expand upon the treatment of riser reconstructions that is outlined in Mériaux et al. [12]; Lensen [41] England and Molnar [13] and Thatcher [15]. In other words, I aim to emphasize epistemic uncertainties associated with fluvial riser reconstructions that have been largely overlooked. Epistemic uncertainty is that which results from a lack of knowledge that leads to multiple viable interpretations of the same data, and contrasts with aleatory uncertainty that results from random measurement errors [42]. Second, and more importantly, I present geomorphic observations that help determine which terrace age most closely approximates the true riser age. Several of these observations are quite important because they invalidate otherwise viable reconstructions and thus reduce epistemic uncertainty. Application of several of these indices to the Cherchen He (River) site along the Altyn Tagh Fault [9] leads to an alternative reconstruction that yields a revised slip rate of 9.4±2.3 mm/yr, consistent with those determined geodetically [1–5] and paleoseismically [6–8]. Without the use of these geomorphic observations, the epistemic uncertainty associated with offset fluvial risers is so large that the presently available data cannot be used to determine whether GPS and geologic slip rates are discrepant within the Indo–Asian collision zone.

2. Potential ambiguity in terrace reconstructions

A flight of fluvial terraces is similar to a set of stairs [43], with terrace *treads* forming gently sloping surfaces separated by steep terrace *risers* formed during incision (Fig. 1A). Each riser separates a younger/lower terrace tread at the *base* of the riser from an older/higher tread at its *crest*. Each tread has a *front* and *back*, corresponding to the edges of the tread that are closest to, and farthest from, the modern stream, respectively. Previous slip-rate studies have focused on the type of terraces flanking the displaced riser. *Fill* terraces form during stream *aggradation* by deposition of alluvium in the channel and subsequent incision to abandon the former floodplain, whereas *strath* terraces are cut into bedrock and form during incision and overall stream *degradation* [44], when the rate of lateral erosion exceeds the rate of vertical incision [45]. How straths form remains an active research subject [46–49]. For present purposes, the *age* of a terrace refers to portions of the tread extending several hundred meters up- and downstream from the fault trace, and refers only to the time at which the tread was abandoned due to renewed incision. This definition of age is independent of whether a terrace is a fill or strath.

In considering how a pair of terrace treads and their intervening riser can be used to determine the rate of strike–slip faulting, it is important to emphasize that two separate records must be used. One record tracks displacement, and starts when the riser begins to accumulate offset. The other tracks age, and starts when a tread is abandoned. Clearly these two separate records must start simultaneously if they are to yield an accurate rate [12]. Thus, the geomorphic and structural evolution of each site must be correctly reconstructed if the age and displacement data are to yield an accurate slip rate. In this way, strike–slip faults contrast with dip-slip faults, where a single terrace tread can be used to measure both the magnitude and age of displacement (e.g., [50–52]).

Early workers in New Zealand recognized potential problems in using terraces to derive slip rates, particularly those resulting from lateral erosion of faulted risers by the active channel before lower-tread abandonment (e.g., [39,41,53]). Lensen [41] provided a particularly

clear conceptual treatment of this problem and demonstrated that five variables are needed (here called D_o, D_u, E, D_a, and D_l). These are defined as follows (see also Fig. 1): D_o is the total observed riser displacement, D_u is the total post-abandonment displacement of the upper tread, and E is the amount of riser offset that is removed by lateral erosion before lower-tread abandonment. The upper tread displacement (D_u) consists of two components, D_a which accumulates after abandonment of the upper tread but before abandonment of the lower tread, and D_l, which accumulates after lower-tread abandonment. Thus, by definition $D_u = D_a + D_l$ and $D_a \geq E \geq 0$. As Lensen [41] demonstrated, a preserved riser displacement (D_o) consists of the total displacement since the upper tread was incised (D_u) minus the amount of lateral erosion (E), such that $D_o = D_u - E = D_a + D_l - E$.

Because the degree of lateral erosion can vary, true displacement/erosion histories can range between the extremes of complete riser refreshment ($E = D_a$; $D_o = D_l$; Fig. 1B and C) to no erosion ($E = 0$; $D_o = D_a + D_l = D_u$; Fig. 1E and F). There are, however, only two abandonment ages to choose from (the top and bottom treads), forcing us to assume an end-member reconstruction to calculate slip rate. In particular, an observed riser offset can be combined with either the abandonment age of the lower tread, herein called the *lower-terrace reconstruction* (Fig. 1A–C) or the age of the upper tread, herein called the *upper-terrace reconstruction* (Fig. 1D–F). The lower- and upper-terrace reconstructions are equivalent to the "strath abandonment" and "fill abandonment" models described by Mériaux et al. [12]. In an attempt to account for accumulation of riser offset prior to abandonment of the lower tread, Mériaux et al. [12] also presented an intermediate reconstruction, the "strath emplacement" model. In this model, the rate is computed using the oldest age from the lower tread under the assumption that this date reflects the time at which the tread first started to form and/or be emplaced. However, this age has no direct bearing on the magnitude of riser erosion (E) prior to lower tread abandonment. The following section explains the end-member lower- and upper-terrace reconstructions to emphasize the importance of choosing the one that most closely approximates the true displacement history and to highlight the need for geomorphic indices to help guide this selection.

3. Competing end-member reconstructions

3.1. Lower-terrace reconstruction

Lower-terrace reconstructions (Fig. 1A–C) are typically used for strath terraces under the assumption that all riser displacement is removed by lateral erosion and scarp refreshment ($E = D_a$) as long as the lower tread is active (e.g., [35,39,45,54]). Thus, riser displacement is presumed to accrue only after the lower-terrace surface has been abandoned ($D_o = D_l$). If this assumption is in error then the calculated rate will be too fast.

A fundamental requirement of the lower-terrace reconstruction is that if risers are to be completely eroded before lower-tread abandonment, then the stream-perpendicular width of the active channel must increase during progressive displacement (Fig. 1B; see also Fig. 3A below). Importantly, the amount of this widening must be equal to, or greater than, the amount of displacement that occurs while the lower tread is active so that $E = D_a$. Lower-terrace reconstructions have been used to derive slip rates for the Altyn Tagh [9], Kunlun [28–30], and Haiyuan [31] faults within the Indo–Asian collision zone, San Andreas Fault in California [32], North Anatolian Fault in Turkey, [33], Septentrional Fault in the Dominican Republic [34], and the Wellington Fault in New Zealand [35].

3.2. Upper-terrace reconstruction

The upper-terrace reconstruction (Fig. 1D–F) assumes that flow over the lower tread is too slow/weak to refresh the riser ($E = 0$), and that riser displacement begins upon initiation of upper-tread incision. If this assumption is in error, then the computed rate is too slow. For an offset riser above an active strath to escape refreshment, the lower tread must be abandoned diachronously, such that ages systematically decrease from the back to the front of the tread. These age gradients should be particularly pronounced within the sheltered corners along the fault scarp (Fig. 1E–F).

There are several reasons to expect upper-terrace reconstructions to be most accurate for some scenarios. In their study of the Altyn Tagh Fault near Aksay, Mériaux et al. [12] showed that slip rates computed using lower-terrace reconstructions are unreasonably high, even though a number of the terraces are straths. Lensen [43] documented a case where the upper-terrace reconstruction is clearly most accurate by using channel offsets to show equal displacements of a riser and its upper tread (i.e., $D_o = D_u$) along the Branch River in New Zealand. Interestingly, some risers at this site require lower-terrace reconstructions because their offsets are matched by channel offsets on the lower tread (i.e., $D_o = D_l$) while others require an intermediate reconstruction, as indicated by $D_u \geq D_o \geq D_l$ [43]. Using flume experiments, Ouchi [55] demonstrated that lateral erosion of offset channel walls is a function of the

balance between the rates of lateral erosion and riser displacement: high rates of slip relative to incision overwhelmed riser erosion such that riser offsets were preserved despite continued flow at their bases. Incised stream channels that are deflected by strike–slip faulting similarly attest to incomplete riser refreshment. Aggrading streams are also unlikely to refresh displaced risers during fill emplacement [12,56].

Inset drainages crossing active strike–slip faults show a spectrum of geometries (Fig. 2) that likely reflect competition between the rates of faulting and erosion. The upper-terrace reconstruction is expected as an intermediate scenario when this full range is considered. Channels that have been completely truncated or "beheaded" by faulting lie at one end of the spectrum (Fig. 2A), reflecting displacements that outpaced the erosion needed to maintain drainage continuity. Deflected channels (Fig. 2B) reflect situations in which lateral erosion is fast enough to preserve channel continuity by removing the scarps that temporarily shutter across the drainage during fault rupture, but not so rapid as to maintain a straight drainage. Drainages in which lateral erosion removes the downstream terrace that is shuttered in front of the active channel without widening of the channel upstream of the fault (Fig. 2C) produce a downstream channel that is wider than that upstream, attesting to incomplete riser refreshment and an upper-tread reconstruction. In contrast, streams along which older risers are displaced, but risers flanking the active channel are not (Fig. 2D), attest to either complete riser refreshment (leading to a lower surface reconstruction), or a lack of surface rupture since the youngest risers formed. Streams with flights of terraces showing no evidence of displacement by active faulting (Fig. 2E) attest to a lack of surface displacement during terrace formation and thus erosion rates that outpace faulting, forming the other end of the spectrum. Ouchi's [55] flume results suggest that the key factor in determining where a channel will fall on this spectrum is the rate of strike–slip faulting relative to the rates of lateral and vertical erosion during formation of the lower terrace, rather than whether or not the terrace is a strath. In this view, displacement rates that are fast enough to outpace lateral erosion will result in incomplete riser refreshment and require an upper-terrace reconstruction, even

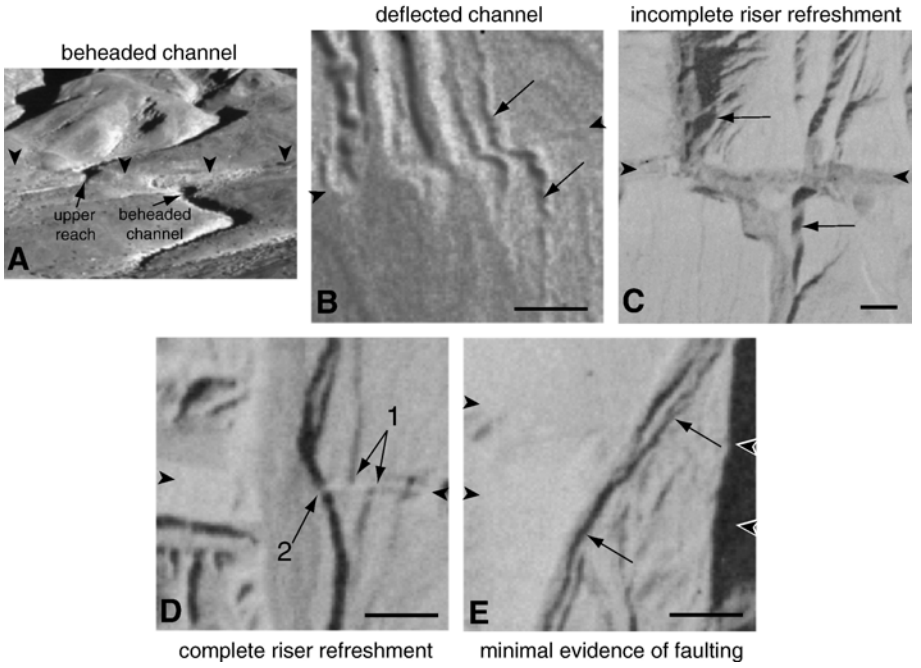

Fig. 2. Examples of stream–fault interactions along Altyn Tagh Fault. Arrowheads delineate fault traces, arrows delineate features mentioned below, and scale bars are 50 m long in panels B–E. Drainage direction is toward bottom of page in all images except D, where it is towards top. Channel responses to active faulting show a spectrum of patterns: (A) complete beheading of a channel that is offset ~18 m from its upper reach (modified from Washburn [66]); (B) deflection of a through going channel (arrowed); (C) riser (arrowed) offsets in excess of the width of the inset channel (supporting an upper-terrace reconstruction, as text and Fig. 3 indicate), (D) upper risers (1) that are displaced but lower risers (2) along the active channel that are not (supporting a lower-terrace reconstruction), and (E) no evidence of riser offset (arrows indicate continuous riser). Panel A shows view to south. North is towards the top of the page in images B–E.

Table 1
Effect of upper-terrace (minimum rate) vs. lower-terrace (maximum rate) reconstruction on calculated slip rate[1]

Site name	Riser name	Offset[2] (m)	Error (m)	UT[3]	UT age[2,3] (yr)	Error (yr)	Min. rate (mm/yr)	Error (mm/yr)	LT[3]	LT age[2,3] (yr)	Error (yr)	Max. rate (mm/yr)	Error (mm/yr)	**Difference factor[4]**	Reference
Altyn Tagh Fault, China															
Cherchen He	T2/T1 (WS)	166	10	T2	16,600	3900	10.0	2.4	T1	6400	70	25.9	1.6	**2.6**	[9]
Cherchen He	T2/T1 (WS)	156	10	T2	16,600	3900	9.4	2.3	T1	6400	70	24.4	1.6	**2.6**	this study
Cherchen He	T2/T1 (ES)	180	10	T2	16,600	3900	10.8	2.6	T1	6400	70	28.1	1.6	**2.6**	[9]
Aksay	T3/T2′ (R2 W bank)	225	10	T3	34,500	2200	6.5	0.5	T2′	9000	1000	25.0	3.0	**3.8**	[12]
Aksay	T3/T2′ (R2 E bank)	220	40	T3	34,500	2200	6.4	1.2	T2′	9000	1000	24.4	5.2	**3.8**	[12]
Aksay	R1, W bank	210	20	T3	34,500	2200	6.1	0.7	T2′	9000	1000	23.3	3.4	**3.8**	[12]
Aksay	R1, E bank	185	20	T3	34,500	2200	5.4	0.7	T2′	9000	1000	20.6	3.2	**3.8**	[12]
Aksay	T2/T1 (Sa1)	145	10	T2	6500	800	22.3	3.1	T1	2200	200	65.9	7.5	**3.0**	[12]
Aksay	T3-T2′/T2 (Sa2)	135	10	T2′	9000	1000	15.0	2.0	T2	6500	800	20.8	3.0	**1.4**	[12]
Aksay	T2′/T2 (Sa1)	165	20	T2′	9000	1000	18.3	3.0	T2	6500	800	25.4	4.4	**1.4**	[12]
Huermo Bulak	T3/T2′-T2 (W R3 total)	275	25	T3	37,900	2800	7.3	0.8	T2′	9000	1000	30.6	4.4	**4.2**	[12]
Huermo Bulak	T2/T1 (total)	125	15	T2	5300	1000	23.6	5.3	T1	2200	200	56.8	8.6	**2.4**	[12]
Huermo Bulak	T2/T1 (E of Sh3)	110	10	T2	5300	1000	20.8	4.3	T1	2200	200	50.0	6.4	**2.4**	[12]
Bang Guo Ba	T3′/T2′ (W of Sb1)	260	30	T3′	29,200	2100	8.9	1.2	T2′	9000	1000	28.9	4.6	**3.2**	[12]
Bang Guo Ba	T2′/T2 (W of Sb1)	165	20	T2′	9000	1000	18.3	3.0	T2	5800	100	28.4	3.5	**1.6**	[12]
Bang Guo Ba	T3 edge (E of Sb1)	240	20	T3	29,200	2100	8.2	0.9	T2	5800	100	41.4	3.5	**5.0**	[12]
Bang Guo Ba	T3 edge (E of R4)	240	20	T3	29,200	2100	8.2	0.9	T2	5800	100	41.4	3.5	**5.0**	[12]
Bang Guo Ba	T2′/T2 (E of R4)	165	20	T2′	9000	1000	18.3	3.0	T2	5800	100	28.4	3.5	**1.6**	[12]
Bang Guo Ba	T3/T2′ (E of Sb2)	215	20	T3	29,200	2100	7.4	0.9	T2′	10,200	1300	21.1	3.3	**2.9**	[12]
Bang Guo Ba	T3/T2′ (W of Sb2)	205	20	T3	29,200	2100	7.0	0.9	T2′	10,200	1300	20.1	3.2	**2.9**	[12]
Bang Guo Ba	T2′/T2 (W of Sb2)	165	20	T2′	9000	1000	18.3	3.0	T2	5800	100	28.4	3.5	**1.6**	[12]
Kunlun Fault, China															
Site 1	T3/T2	33	4	T3	5106	290	6.5	0.9	T2	2914	471	11.3	2.3	**1.8**	[29]
Site 1	T2/T1	24	3	T2	2914	471	8.2	1.7	T1	1778	388	13.5	3.4	**1.6**	[29]
Site 2	T5/T4	110	10	T5	12,614	2303	8.7	1.8	T4	8126	346	13.5	1.4	**1.6**	[28]
Site 2	T4/T3	70	5	T4	8126	346	8.6	0.7	T3	6276	262	11.2	0.9	**1.3**	[28]
Site 3	T3-2/T3-1	47	5	T3-2	6043	553	7.8	1.1	T3-1	4837	857	9.7	2.0	**1.2**	[28]
North Anatolian Fault, Turkey															
Üçoluk River	T1/T2	34	3.5	T1	3970	80	8.6	0.9	T2	1640	60	20.7	2.3	**2.4**	[33]
Calaveras Fault, USA															
Welch Creek	Qt3/Qt4	39	1	Qt3	13,120		3.0		QT4	4985		7.8		**2.6**	[57]

for straths. This suggestion is supported by the observation that most of the displaced risers reported from New Zealand and for which tread offsets are independently known follow the lower-terrace reconstruction [54] because the drainages flanking these straths are generally large, permanent rivers along which the rate of lateral erosion is likely high relative to that of faulting. In contrast, the small-discharge, ephemeral streams that are common along central Asian strike–slip faults are likely to have lower rates of erosion relative to displacement, favoring incomplete riser refreshment [12]. As a result, it is dangerous to simply assume that a riser must follow the lower-terrace reconstruction because it is a strath.

3.3. Impact on computed slip rate

Table 1 demonstrates the potential impact of site reconstruction on the rate of strike–slip faulting derived from an offset riser. In the table, published riser offsets and terrace ages are compiled for several major fault systems, but only include those sites for which rates were determined using displaced risers and ages were also reported for both the upper and lower flanking terraces. Although in some cases the minimum and maximum slip rates derived from these data differ by as little as a factor of 1.2, for most sites the difference is considerably larger, and in some cases is as large as a factor of 5. Thus, the epistemic uncertainty associated with current methods for determining slip rate from offset fluvial risers is likely to be so large that either there is no discrepancy between the GPS and geologic rates within the Indo–Asian collision zone (e.g., [13,15]), or if there is such a divergence, it cannot be resolved with current data.

Clearly the structural and geomorphic evolution of an offset riser must be correctly determined to reduce the epistemic uncertainty and establish an accurate slip rate. The most conservative approach for dealing with this problem is that shown in Table 1, which is to date both treads and then calculate minimum and maximum rates using the upper and lower tread ages, respectively (e.g., [12,33,57]). However, this approach must be refined to narrow the range and determine slip rates as accurately as possible.

4. Geomorphic indices for resolving ambiguity

At least six indices can be used to guide accurate reconstructions of fluvial risers (Fig. 3). These criteria are presented in decreasing order of utility, followed by a comparison of their relative usefulness.

4.1. Riser offset versus inset channel width

The first index compares the riser offset with the width (and/or offset) of the main channel that is incised into the lower tread (Fig. 3A). Once the lower tread is abandoned, the new channel will match all offset of the riser above the tread by either widening or becoming offset. If the riser at the back of the lower tread was completely refreshed prior to lower-tread incision, then the offset and/or width of the inset channel must be *equal to or greater than* the magnitude of this riser offset. Thus, riser displacements exceeding the width and/or offset of the channel cut into their lower tread must have accumulated prior to formation of the inset channel, and therefore attest to incomplete riser refreshment. Examination of stereo-imagery along the Altyn Tagh Fault indicates that riser offsets commonly exceed inset valley widths/offsets where the drainage upstream from the fault is confined within a narrow canyon, presumably because the canyon limits the extent to which the stream can widen and refresh the risers. The difference between the riser offset and the inset channel width provides a minimum estimate for the amount of residual riser offset that existed prior to lower-tread abandonment.

4.2. Similarity of riser and tread displacements

The second index follows Lensen [41,43], who showed that a robust way of choosing a reconstruction is to compare the observed riser offset (D_o) with offsets of primary features on the upper (D_u) and lower (D_l) treads (Fig. 3B) [41,43]. Primary features are inherited from the time the tread was abandoned and can include channels,

Notes to Table 1:

[1]Comparisons are made only for fluvial terrace risers for which both upper and lower-terrace ages are reported. Although the Karakoram Fault has been argued to show variable slip rate [11] and GPS and geologic rates for the Haiyuan fault appear discrepant [15], data for these faults are not included because in the first case the rates are derived from offset moraines rather than fluvial risers, and in the second case, upper-terrace ages were not reported.

[2]Offset and age values are those used in original publications for slip-rate determinations. Alternative interpretations of the data are not considered here.

[3]UT is upper terrace and LT is lower terrace.

[4]Difference factor is maximum rate divided by minimum rate, and demonstrates the impact on the reported slip rate of the model used to reconstruct the site.

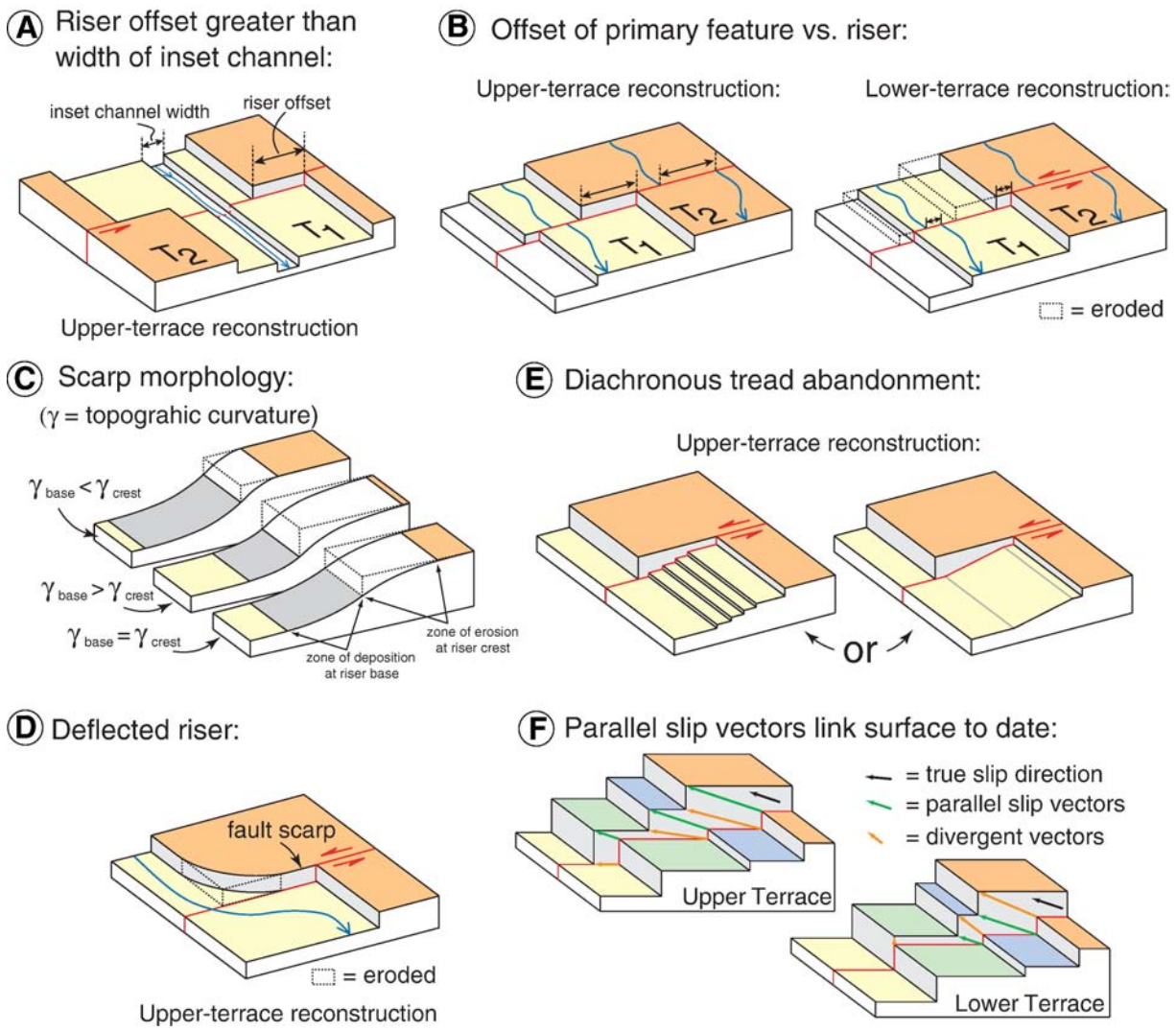

Fig. 3. Geomorphic indices for evaluating suitability of upper- vs. lower-terrace reconstruction. See text for explanation. (A) Magnitude of riser offset relative to width of channel inset into lower tread; (B) magnitude of riser offset relative to displacement of primary features (e.g., relict channels) on tread surface; (C) scarp morphologies. Bottom profile shows a symmetric scarp resulting from diffusion, middle profile shows an asymmetric scarp with a low curvature crest and high curvature base resulting from removal of material from the toe of the scarp during partial riser refreshment, top profile shows an asymmetric scarp with a high curvature crest and a low curvature base resulting from addition of loess and/or the presence of a cohesive unit in the upper terrace. (D) Abrupt truncation vs. curved riser at intersection with fault; (E) isochronous vs. diachronous tread ages; and (F) parallelism of vectors linking riser crests and bases.

debris-flow margins, alluvial fans, or moraines. In the case of complete riser refreshment ($E=D_a$), the riser and primary features on the lower tread will be offset the same (i.e., $D_o=D_l$), with features on the upper tread recording larger displacements ($D_u>D_o$). In contrast, in the case of no riser refreshment ($E=0$) the riser and upper tread will show the same offset ($D_o=D_u$) and exceed displacements on the lower tread ($D_o>D_l$). Such differences will not develop if incision and terrace formation outpaced the rate of displacement, so that displacements of the upper and lower treads are equal ($D_o=D_u=D_l$) (e.g., [58,59]). In this case the abandonment age of the lowermost tread provides a minimum slip rate because the offset happened after its abandonment.

4.3. Morphologic dating of risers

A third index uses the morphology of the riser measured in topographic profiles orthogonal to the riser scarp (Fig. 3C). By assuming that mass transport is

linearly proportional to the local topographic slope and that mass is locally conserved (i.e., the scarp is non-cohesive and not dissected), the age of the scarp can be estimated by using the diffusion equation to model the topographic evolution of the riser as it degrades (e.g., [42] and references therein, [60] and references therein). A number of studies have used this approach to date fluvial risers (e.g., [61–65]). Importantly, to determine the time (t) of riser formation, the mass diffusivity (κ) must also be known, otherwise only a diffusivity age (κ multiplied by t) can be determined. Scarp morphology can be used in at least three ways to help guide terrace reconstructions. First, the age of the riser can be determined directly, circumventing the need to use one of the tread area as a proxy, if κ is known and the scarp is symmetric (i.e., the curvature of eroding riser crest is equal to the curvature of the depositional surface at the riser base, Fig. 3C, lowermost profile). Second, the form of the topographic profile can be used to identify incomplete refreshment: lateral erosion of the riser base after the scarp has started to degrade should produce a scarp with a diffused, low curvature riser crest but a steeper, higher curvature base (Fig. 3C, middle profile). Third, diffusivity ages that vary significantly along the length of the riser can indicate complete but spatially localized scarp refreshment.

4.4. Riser deflections

A fourth index is whether risers are abruptly truncated or curved where they intersect the fault (Fig. 3D). A curved riser is one for which the acute angle between the riser and the fault trace decreases systematically as the riser approaches the fault. Such geometry implies either that the fault happened to cut a pre-existing meander bend in the riser, or that the riser was incompletely refreshed prior to lower-tread abandonment. When a fault rupture crosses an active stream and left-laterally displaces risers on either side of the channel it will form fault scarps that face downstream on the left bank and upstream on the right bank when looking downstream. Repeated ruptures will shutter these scarps across the active stream, narrowing the channel where it crosses the fault. The curved riser develops when the stream partially erodes these scarps (Fig. 3D). Curved risers support an upper-terrace reconstruction because they attest to incomplete riser refreshment.

4.5. Diachroneity of terrace abandonment

A fifth index is the extent to which tread abandonment is diachronous (Fig. 3E). Because the lower-terrace reconstruction presumes that all riser offsets are removed prior to lower-tread abandonment, it requires the active channel to migrate from bank to bank rapidly relative to the displacement rate (Fig. 1B). Frequent tread occupation should produce a surface that is abandoned roughly isochronously. By contrast, tread abandonment is diachronous in the upper-terrace reconstruction. Specifically, the portions of the lower tread that lie within the sheltered corners (Fig. 1F) are transported away from the active channel during strike–slip faulting and therefore should show systematic age progressions roughly orthogonal to the riser, with the oldest portions of the tread lying at the back of the terrace. Relative tread ages can be established using vegetation size/density, soil/varnish development, or the degree of channel-bar preservation. Flights of small terraces that progressively step down from the back to the front of a tread, or a tread that slopes towards the active channel may also attest to diachronous abandonment (Fig. 3E). Tread diachroneity can also be determined using ^{14}C or cosmogenic-nuclide ages. Van der Woerd et al. [28] reported a possible ~1000-yr reduction in Berillium-10 (^{10}Be) ages from the back to front of the treads at Site 1 along the Kunlun Fault, and suggested this variation might reflect diachronous tread abandonment. An upper-terrace reconstruction of at Site 1 (Table 1) yields rates of 6.5 (T3/T2) and 8.2 mm/yr (T2/T1), which should be more accurate than 11.3 and 13.5 mm/yr as reported by Van der Woerd et al. [28], who used a lower-terrace reconstruction.

4.6. Parallelism of riser crest/base offsets and the slip vector

A sixth index is whether riser crests or bases yield the slip vector (Fig. 3F). This index requires that fault slip was oblique, so that the riser and active tread undergo vertical and lateral displacement. In this situation, complete refreshment of both the riser and active tread will produce a line of intersection between the riser face and the active tread that is continuous across the fault when the lower tread is abandoned. This piercing line will record fault motion subsequent to its formation. In contrast, the riser crests form a spurious piercing line because vertical separation of the upper tread and lateral erosion of the riser face produces crests that were never colinear. The opposite pattern holds if the riser offset is preserved but the vertical offset of the tread is removed by erosion/deposition, so that the riser crest forms a piercing line and the base is spurious. These relationships can be used to distinguish between upper- and lower-terrace

reconstructions in two ways. First, if the slip direction is known independently and matches the vector linking the riser bases, then the lower-terrace reconstruction should be used. Likewise, the upper-terrace reconstruction is needed if the riser crests yield the slip vector. The second situation applies to a set of degradational terraces that formed under conditions of uniform riser erosion and slip direction. In this situation a lower-terrace reconstruction is indicated if a parallel set of vectors link the riser bases, whereas an upper-terrace reconstruction is needed if the parallel vectors link the riser crests.

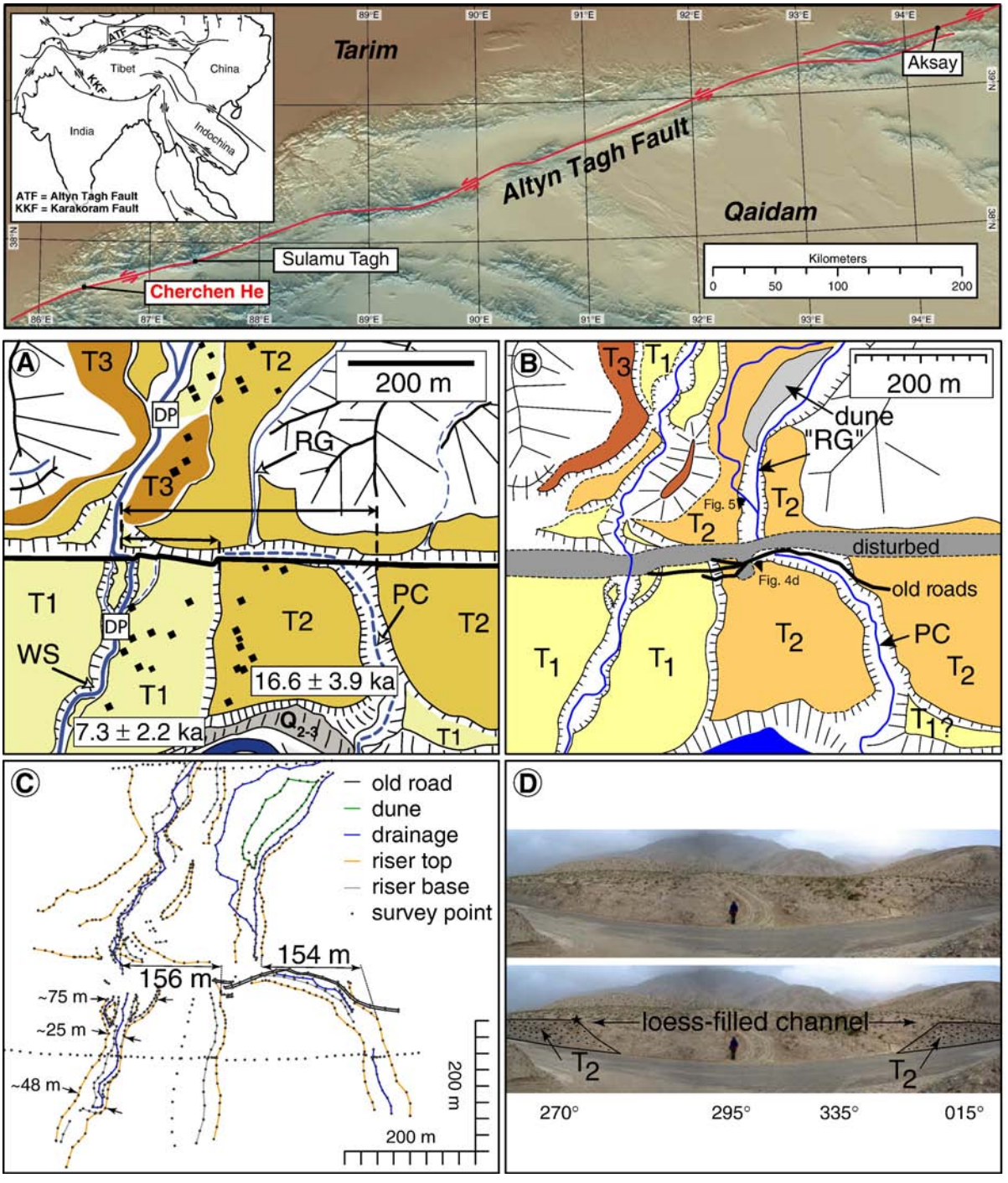

4.7. Relative usefulness of the indicators

Of the six geomorphic indicators described above, the first three are particularly important because they can be used to eliminate possible reconstructions. The inset channel width index described in Section 4.1 is particularly robust, and has the advantage of being both common and easy to document. Riser offsets larger than the width of the channel inset into their lower-terrace tread clearly attest to riser offset prior to inset channel formation, generally invalidating the end-member lower-terrace reconstruction. As demonstrated below (Section 5), the difference between the magnitude of riser offset and the inset channel width provides a minimum estimate for the amount of riser offset that predates lower-tread abandonment. Although there are two situations in which this index breaks down, both are likely to be rare. First, if drainage across the lower tread ceases, then riser offset can accrue after the lower tread has been abandoned but before it has been incised. Such behavior is unlikely, however, because tread-modifying discharge events are likely to occur more frequently than surface-rupturing earthquakes. Second, if an initial channel inset in the lower tread is backfilled and then a new inset channel forms, then the inset channel width can be smaller than the riser offset. However, such backfilling must be just sufficient to hide the earlier channel without resurfacing the flanking tread so that the lower tread abandonment age remains unperturbed.

As Section 4.2 indicates, riser offsets that are equivalent to offset primary features on an adjacent tread clearly refute models using the other tread age. Although the tread-displacement index is particularly robust, its applicability is limited by the paucity of primary features on displaced treads and the difficulty of establishing that such markers date from the time of tread abandonment. Use of the scarp morphology to directly date the time of riser abandonment (Section 4.3) circumvents the need to use a terrace tread age as proxy, and thus is a potentially powerful tool in analysis of offset risers. Unfortunately, use of scarp morphology to date risers can be limited by several factors, although recent work integrating morphologic modeling with cosmogenic nuclide measurements [38] shows considerable promise. The most important limitation is that the uncertainties of scarp ages determined using morphologic analysis are typically large (e.g., 25–70% in cases reviewed by Hanks [42]), and thus may not provide sufficient resolution to discriminate between upper and lower-terrace reconstructions. For many of the sites reported in Table 1, 50% errors in the ages would yield overlapping upper and lower-terrace ages. Loess accumulation (e.g., [62]) or the presence of consolidated material (e.g., caliche or bedrock) beneath the upper tread can produce an asymmetric scarp with a lower curvature base and a higher curvature crest (Fig. 3C, top profile), complicating the morphologic analysis [60] and increasing the uncertainty in the derived riser age. Because fluvial terrace risers trend down regional slopes, transport of material in and out of the plane of the topographic profile should also be considered. Finally, uncertainty in the initial slope of the scarp will also propagate into uncertainty in the scarp age.

Although the last three indices (riser deflections, diachronous tread abandonment, riser offsets parallel to slip direction) can be used to support a proposed reconstruction, they can form by other processes and thus can rarely be used to invalidate reconstructions. For example, riser deflections (Section 4.4) can form by a meandering channel. Thus, this observation can only refute the end-member lower-terrace reconstruction in situations where the risers being transported into the stream by strike–slip motion (i.e., "leading" risers [45]) are curved while those that are being transported away from the stream by strike–slip motion (i.e., "trailing" risers [45]) are straight. Likewise, diachronous tread abandonment (Section 4.5) can result simply from the

Fig. 4. New data from Cherchen He site of Mériaux et al. [9]. Geomorphic indices at this site indicate upper-terrace reconstruction is most appropriate, yielding a slip rate of 9.4±2.3 mm/yr. To calculate this rate I used the published abandonment age for the upper (T2) terrace and my revised T2/T1 offset. The estimated uncertainty of 2.3 mm/yr is based only on the uncertainties in the age and offset measurements and does not include uncertainty in the reconstruction (i.e., epistemic uncertainty). Top panel shows active trace of the Altyn Tagh Fault and locations of the Cherchen He, Sulamu Tagh, and Aksay Sites. Inset shows a simplified map of the major faults in the Indo–Asian collision zone with a box outlining the Altyn Tagh Fault map. Panels A–D show data from Cherchen He. (A) Portion of original site map showing ^{10}Be exposure ages (cropped from Fig. 2B of [9]). (B) New neotectonic map based on field observations and survey data collected in 2005. Gray band along Altyn Tagh Fault approximately delineates area disturbed by new road construction. Bold black lines indicate old roads cutting T2/T1 riser (see also Fig. DR1). Note dune of loess and width of "RG" channel. Basemap was an unrectified portion of CORONA image DS1025-2118DA031 scanned at ~2.5 m/pixel. No measurements are reported from this map due to lack of orthorectification. (C) New survey data from Cherchen He used to determine offset magnitudes and channel widths. Survey data were gathered using a Leica TR407power total station following methods described in Cowgill et al. [67] and Gold et al. [68]. These data indicate offsets of 156±10 m and 154±10 m for the top of the T2/T1 riser and east bank of "RG"–PC, respectively. (D) Photo-mosaic of exposure of the "RG" drainage created by new road construction. Width of loess-filled channel in T2 terrace is much larger than modern gulley incised into this loess fill. Star denotes intersection of west bank of buried channel with T2 surface. This contact is exposed on the T2 surface north of the road cut (Fig. 5) and was used in the map (Fig. 4B) and survey (Fig. 4C) to delineate the original width of "RG" prior to its burial by loess. For scale, person is 1.8 m tall.

lateral migration or intermittent occupation of the active channel. Diachronous abandonment can also be difficult to establish conclusively. Finally, the slip-vector index (Section 4.6) may be difficult to apply because it requires accurate riser offset measurements that may be obscured by modification of the riser crests and bases by erosion and burial, respectively. In addition, this index is predicated on several important assumptions that may be difficult to assess.

5. Implications

To illustrate how the above geomorphic indices can be applied, consider the Cherchen He site along the Altyn Tagh Fault in northwestern China (Fig. 4, DR1–6). At this site, Mériaux et al. [9] assumed a lower-terrace reconstruction and determined a rate of 25.9±1.6 mm/yr by combining a 166±10 m displacement of the T2/T1 terrace riser with an age of 6.4±0.07 ka for the T1 strath (Fig. 4A). This age was determined using ^{14}C and is supported by ^{10}Be clast ages from the tread surface that give an age of 7.3±2.2 ka (Fig. 4A). A similar rate of 25.2±5.9 mm/yr was determined by restoring a channel (PC) on the T2 surface by 418±20 m back to the main drainage (WS) (Fig. 4A), and combining this offset with an average ^{10}Be exposure age of 16.6±3.9 ka for the T2 surface. Mériaux et al. [9] proposed a minimum slip rate for the Cherchen He site of 16.6±1.5 mm/yr by combining the T2/T1 riser offset with the youngest ^{10}Be age (10±0.71 ka) from the upper T2 surface. This is unlikely to be a true minimum estimate because most post-emplacement modification of terrace deposits will result in ^{10}Be apparent ages that underreport the true age (e.g., [10,14,37]) and thus rates that are higher than the true value.

New maps and field observations of the Cherchen He site (Figs. 4B–D, 5 and DR2-6) reveal geomorphic observations that either refute or fail to support a lower-terrace reconstruction of this site and indicate that an upper-terrace reconstruction is most appropriate. Three observations are particularly important: (1) the offset of the T2/T1 riser is larger than the width of the channel inset into the T1 tread (first index, Fig. 3A), (2) a primary feature on the T2 tread (PC) shows an offset that is equal to the T2/T1 riser offset (second index, Fig. 3B), and (3) the T2/T1 riser on the west side of WS is deflected on the upstream side of the fault but is straight on the downstream side (fourth index, Fig. 3D). The upper-terrace reconstruction of the Cherchen He site yields a slip rate that is equivalent within error to those derived using GPS and paleoseismic techniques elsewhere along the fault.

By far the most important new observation from the Cherchen He site is that the magnitude of T2/T1 riser is 2–6 times larger than the width of the channel inset into the T1 tread. The new survey data (Fig. 4C) yield a revised total offset of 156±10 m for the T2/T1 riser from the east bank of the WS drainage. In contrast, the channel inset into the T1 tread is only 25 to 48 m wide along most of its length, reaching a maximum width of 75±10 m within 100 m south of the fault (Fig. 4C). Thus, the T1 surface can have been displaced no more than 75 m since the stream started incising the active channel into T1, indicating that at least 81 m (156–75 m) of T2/T1 riser offset must have accrued prior to formation of the active channel. An end-member lower-terrace reconstruction thus is clearly refuted for this site because otherwise the T1 surface would have had to remain unmodified for ~3000 yr before being incised to form the active channel. In addition, the uniform texture of the T1 surface argues against their being an older channel that was backfilled just to the level of the T1 surface prior to incision of the present inset channel. Using the abandonment age for the upper (T2) terrace and the revised T2/T1 offset reported here, I calculate a revised slip rate of 9.4±2.3 mm/yr, the estimated uncertainty of which is based only on the aleatory uncertainties in the age and offset measurements. Likewise, using the T1 abandonment age and the inset channel width of 75±10 m yields a slip rate of 11.7±1.6 mm/yr.

In contrast to the original reconstruction, in which the PC drainage was restored to the WS [9], additional new observations indicate that PC is best restored to the "RG" channel to the north. Thus, the "RG"–PC drainage appears to form a primary feature on the T2 tread for comparison with the T2/T1 riser offset (second index, Fig. 3B). The supplementary material provides additional discussion of this alternative reconstruction. The "RG" channel was originally interpreted as a younger regressive gulley because the modern "RG" channel is narrower than the PC valley to the south of the fault (e.g., Fig. 4A) [9]. However, exposures produced during new road construction in July, 2005 reveal that the "RG" channel is partially filled by loess, explaining its narrower appearance (Fig. 4D). Where the loess-covered western bank of the "RG" channel intersects the T2 tread at the top of the road cut, the T2 surface preserves a gradational but localized contact between a cobble-covered surface to the west and the younger loess deposited within the "RG" channel (Fig. 5). This contact was surveyed to map the western edge of the "RG" channel (Fig. 4B–C). Thus, both the road cut (Fig. 4D) and survey data (Figs. 4C and 5) clearly show that the

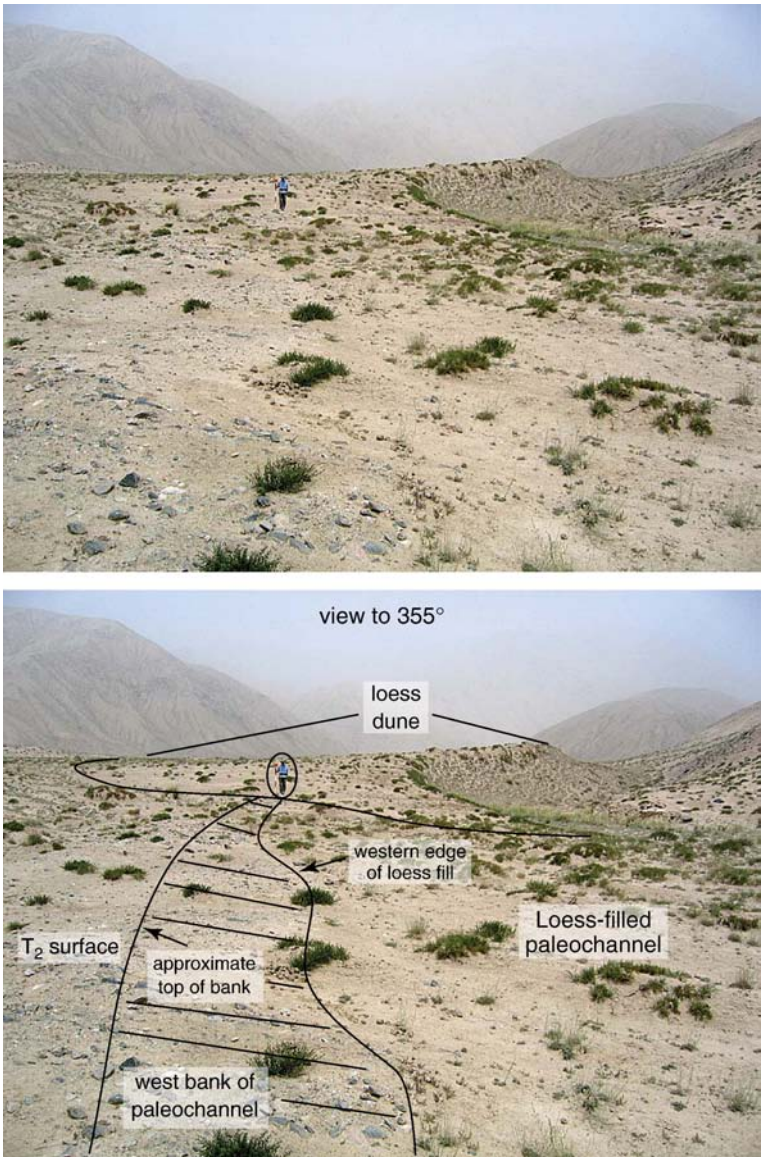

Fig. 5. Western bank of "RG" drainage, looking upstream (north). See Fig. 4 for locations of "RG" channel, loess dune, and photo shown here. A) Original and B) interpreted field photos showing western edge of "RG" channel, partially concealed by loess, with loess dune in distance. Note the paucity of cobbles within the loess-filled channel on the right (east) relative those on the exposed T2 tread to the left (west). For scale, circled person is 1.8 m tall. Photo taken Aug. 5, 2005.

true width of the "RG" channel is similar to that of the PC channel south of the fault.

The PC was also originally restored to the WS because the PC was mapped as continuing west of the RG channel to the T2/T1 riser (Fig. 4A), indicating deflection of the PC–WS channel until PC abandonment during T2/T1 riser formation [9]. However, an old road along the proposed extension of the PC west of the "RG" channel lies only ~1 m below the elevation of the T2 tread (Figs. DR3–5), which appears too high for the PC channel to have been present in this region. The old road network had also breached the T2/T1 riser in at least 3 points. Thus, the simplest interpretation is that the T2 tread and T2/T1 riser edge have been lowered by human activity along an old road/trail network and that the western edge of the PC was a continuation of the western edge of the "RG" channel. Restoration of the east bank of the PC–"RG" drainage yields a displacement of 154±10 m, equivalent to the T2/T1 riser offset of 156±10 m (Fig. 4C), supporting

my interpretation of the PC–"RG" drainage as an offset primary feature and leading to an upper-terrace reconstruction as described in Section 4.2. Combining this revised offset with the published T2 ^{10}Be exposure age yields a rate of 9.3±2.3 mm/yr. Final support for an upper-terrace reconstruction comes from the observation that the T2/T1 riser on the east bank of WS curves into the trace of the fault (Fig. 4A–C), whereas to the south of the fault it is straight, consistent with incomplete riser refreshment prior to T1 abandonment (e.g., Fig. 3D and Section 4.4).

Is this alternative reconstruction of the Cherchen He site consistent with results from the other sites along the central Altyn Tagh Fault? At the Sulamu Tagh site (~87.4° E), a series of glacial features were dated using climatic correlations and ^{10}Be model ages. The three best-constrained slip-rate determinations were derived from 1) a glacial confluence displaced 3660±300 m and interpreted to have formed at 112.7±7.3 ka on the basis of the oldest ^{10}Be age found in glacial till blanketing the confluence, 2) a channel displaced 2080±100 m and interpreted to have formed at 66.2±1.8 ka based on four ^{10}Be model ages from clasts on the channel floor, and 3) a moraine displaced 1400±100 m and dated at 47.1±4.4 ka on the basis of five ^{10}Be model ages from clasts within the moraine [9]. Alternative interpretations of the Sulamu Tagh data that permit slip rates of ~10 mm/yr are also possible because this interpretation of the site is not unique [9]. In particular, the glacial confluence could have been excavated at ~350 ka, rather than at ~112 ka, and the channel and moraine could have formed at ~210 ka and ~140 ka, respectively, by glacial reoccupation of drainages that had already been deflected along the trace of the fault.

Although the revised slip rate proposed here is compatible with the data from Sulamu Tagh, it does conflict with the average Holocene rate of 17.8±3.6 mm/yr reported from three sites near Aksay (~94° E) [12]. The Aksay rates were derived largely using upper-terrace reconstructions and thus should be minimum rates. At least two scenarios can explain this discrepancy. One possibility is that the slip rate on the Altyn Tagh Fault has varied several times, being slow prior to ~10 ka, as indicated by the revised Cherchen He data, fast from ~10 to 2 ka to accommodate the Aksay data, and then slow from ~1 ka to present to fit the geodetic and paleoseismic results. Slow rates (~6.5 mm/yr) at Aksay derived from upper-terrace reconstructions of risers inset into Late Pleistocene terraces are broadly consistent with this scenario. The other possibility is that the rates reported from Aksay are too high, either because of systematic errors in the way the terrace ages that were used to compute the slip rates were derived from the ^{10}Be and ^{26}Al model ages, or because of errors resulting from extrapolation of the terrace ages to offset markers that were not directly dated. Clearly, additional work is needed.

6. Conclusions

Slip-rate data appear to be in conflict for several of the first-order strike–slip faults within the Indo–Asian collision, reflecting either true secular variation in slip rate or errors in how the rates were determined, or both. Although recent attention has focused primarily on the interpretation of the age data [10,13,14], potentially critical ambiguities regarding the geomorphic reconstruction of displaced fluvial terraces have not previously been discussed in detail. To derive a slip rate from a displaced fluvial riser, two end-member reconstructions are possible. The lower-terrace reconstruction yields a maximum rate by assuming that stream flow on the lower tread completely refreshes the riser such that offset does not begin to accrue until the lower surface is abandoned (i.e., $E=D_a$ such that $D_o=D_l$ and $D_u>D_o$). The alternative, upper-terrace reconstruction provides a minimum rate by assuming that riser offset starts accumulating as soon as the riser forms by incision of the upper tread (i.e., $E=0$ such that $D_o=D_u=D_a+D_l$).

In reality, most cases likely fall between these two extremes (i.e., $D_a>E>0$), but we are generally forced to use end-member reconstructions because we typically have only two tread abandonment ages for any one offset terrace riser. As the data summarized in Table 1 indicate, an offset fluvial riser can lead to a maximum slip rate that is as much as 5 times faster the minimum rate, if the geomorphic observations presented above are not used to reduce this epistemic uncertainty. Thus, it is essential to choose the end-member reconstruction that most closely approximates the true history. At least six geomorphic relationships attest to incomplete riser refreshment. (1) Riser offsets that are larger than the width of the channel that is inset into the lower tread; (2) riser offsets that are equivalent to the displacement of primary features (e.g., stream channels) on the upper tread surface and larger than those on the lower tread; (3) riser scarps that predate lower-terrace abandonment, as determined by morphological age analysis; (4) risers that deflect where they intersect the fault, but that match with a straight riser on the opposite side of the fault; (5) diachronous lower tread abandonment with ages that systematically young from the riser to the active channel; and (6) riser crests and bases that yield parallel and diverging slip vectors, respectively. These indices are important both for evaluating previously published slip-

rate sites and for minimizing epistemic uncertainty in future investigations. Without the use of geomorphic observations such as these, the epistemic uncertainty associated with determining slip rates from offset fluvial risers is so large that there is no resolvable discrepancy between the GPS and geologic rates within the Indo–Asian collision zone (e.g., [13,15]).

New mapping, survey data, and excavations from the Cherchen He site along the Altyn Tagh Fault indicate that the previously published rates for this site are too high because they are based on a lower-terrace reconstruction that is incompatible with the site geomorphology. Specifically, I find the T2/T1 riser is displaced 156±10 m, which is 2–6 times larger than the width of the channel that is inset into the T1 tread at the base of the riser. As the first index demonstrates, this relationship is incompatible with the lower-terrace reconstruction and indicates that at least 81 m of the observed riser offset had accumulated prior to incision of the T1 tread. Application of an upper-terrace reconstruction to these data yields a revised rate of 9.4±2.3 mm/yr. Likewise, new road cuts and detailed mapping of the T2 surface indicate that the width of the "RG" channel upstream of the fault is greater than previously presumed and is equivalent to the PC drainage south of the fault. The eastern margin of the "RG"–PC drainage is offset 154±10 m, yielding a revised rate of 9.3±2.3 mm/yr. These revised rates are consistent with those determined geodetically [1–5] and paleoseismically [6–8], suggesting that the apparent discrepancy in slip rate along this fault might result more from systematic biases in geomorphic reconstructions rather than from true secular variation in slip rate.

Acknowledgements

This project was supported by the UC Davis New Faculty Research Grant Program and by NSF grant EAR-0610107 from the Tectonics Program and the East Asia and Pacific Program in the NSF Office of International Science and Engineering. I thank Ryan Gold for his helpful discussions on riser reconstructions and for his help in preparing initial drafts of Figs. 1 and 4B. Discussions with Ramon Arrowsmith, Adam Forte, Nick Raterman and Amanda Tyson were also very helpful. Ryan Gold, Amanda Tyson, Jiang Rongbao, Chen Xuanhua, and Wang Xiao-feng helped with fieldwork and associated logistics. An early draft of the manuscript benefited from reviews by Ryan Gold and Amanda Tyson. I thank Tom Hanks, Wayne Thatcher, and Peggy Delaney (editor) for their very constructive reviews.

Appendix A. Supplementary data

Supplementary data associated with this article can be found, in the online version, at doi:10.1016/j.epsl.2006.09.015.

References

[1] R. Bendick, R. Bilham, J. Freymueller, K. Larson, G. Yin, Geodetic evidence for a low slip rate in the Altyn Tagh fault system, Nature 404 (2000) 69–72.
[2] Z.-K. Shen, M. Wang, Y. Li, D.D. Jackson, A. Yin, D. Dong, P. Fang, Crustal deformation along the Altyn Tagh fault system, western China, from GPS, J. Geophys. Res. 106 (12) (2001) 30,607–30,621.
[3] Z. Chen, B.C. Burchfiel, Y. Liu, R.W. King, L.H. Royden, W. Tang, E. Wang, J. Zhao, X. Zhang, Global positioning system measurements from eastern Tibet and their implications for India/Eurasia intercontinental deformation, J. Geophys. Res. 105 (7) (2000) 16,215–16,227.
[4] K. Wallace, G. Yin, R. Bilham, Inescapable slow slip on the Altyn Tagh fault, Geophys. Res. Lett. 31 (L09613) (2004), doi:10.1029/2004GL019724.
[5] P.-Z. Zhang, Z. Shen, M. Wang, W. Gan, R. Bürgmann, P. Molnar, Q. Wang, Z. Niu, J. Sun, J. Wu, H. Sun, X. You, Continuous deformation of the Tibetan Plateau from global positioning system data, Geology 32 (9) (2004) 809–812, doi:10.1130/G20554.1.
[6] Z. Washburn, J.R. Arrowsmith, S.L. Forman, E. Cowgill, X. Wang, Y. Zhang, Z. Chen, Late Holocene earthquake history of the central Altyn Tagh Fault, China, Geology 29 (11) (2001) 1051–1054.
[7] Z. Washburn, J.R. Arrowsmith, G. Dupont-Nivet, X.-F. Wang, Y.-Q. Zhang, Z. Chen, Paleoseismology of the Xorxol segment of the Central Altyn Tagh Fault, Xinjiang, China, Ann. Geophys. 5 (2003) 1015–1034.
[8] S. Ge, G. Shen, R. Wei, G. Ding, Y. Wang, The Altyn Tagh Active Fault System, State Seismological Bureau of China, Beijing, P.R. China, 1992 (in Chinese with English abstract), 319 pp.
[9] A.-S. Mériaux, F.J. Ryerson, P. Tapponnier, J. Van der Woerd, R.C. Finkel, X. Xu, Z. Xu, M.W. Caffee, Rapid slip along the central Altyn Tagh Fault: morphochronologic evidence from Cherchen He and Sulamu Tagh, J. Geophys. Res. 109 (B06401) (2004), doi:10.1029/2003jb002558.
[10] E.T. Brown, R. Bendick, D.L. Bourlès, V. Gaur, P. Molnar, G.M. Raisbeck, F. Yiou, Slip rates of the Karakorum fault, Ladakh, India, determined using cosmic ray exposure dating of debris flows and moraines, J. Geophys. Res. 107 (B9) (2002) 2192, doi:10.1029/2000JB000100.
[11] M.-L. Chevalier, F.J. Ryerson, P. Tapponnier, R.C. Finkel, J. Van der Woerd, H. Li, Q. Liu, Slip-rate measurements on the Karakorum fault may imply secular variations in fault motion, Science 307 (2005) 411–414.
[12] A.-S. Mériaux, P. Tapponnier, F.J. Ryerson, X. Xu, G. King, J. Van der Woerd, R.C. Finkel, H. Li, M.W. Caffee, Z. Xu, W. Chen, The Aksay segment of the northern Altyn Tagh fault: tectonic geomorphology, landscape evolution, and Holocene slip rate, J. Geophys. Res. 110 (B04404) (2005), doi:10.1029/2004JB003210.
[13] P. England, P. Molnar, Late Quaternary to decadal velocity fields in Asia, J. Geophys. Res. 110 (B12401) (2005), doi:10.1029/2004JB003541.

[14] E.T. Brown, P. Molnar, D.L. Bourlés, Comment on "Slip-rate measurements on the Karakorum Fault may imply secular variations in fault motion", Science 309 (2005) 1326b.
[15] W. Thatcher, Microplate model for the present-day deformation of Tibet, J. Geophys. Res. (in press).
[16] S.J. Kenner, M. Simons, Temporal clustering of major earthquakes along individual faults due to post-seismic reloading, Geophys. J. Int. 160 (1) (2005) 179–194.
[17] Y. Ben-Zion, K. Dahmen, V. Lyakhovsky, D. Ertas, A. Agnon, Self-driven mode switching of earthquake activity on a fault system, Earth Planet. Sci. Lett. 172 (1999) 11–21.
[18] J. Chéry, P. Vernant, Lithospheric elasticity promotes episodic fault activity, Earth Planet. Sci. Lett. 243 (2006) 211–217.
[19] A.M. Friedrich, B.P. Wernicke, N.A. Niemi, R.A. Bennett, J.L. Davis, Comparison of geodetic and geologic data from the Wastach region, Utah, and implications for the spectral character of Earth deformation at periods of 10 to 10 million years, J. Geophys. Res. 108 (B4) (2003) 2199, doi:10.1029/2001JB000682.
[20] N. Ambraseys, Value of historical record of earthquakes, Nature 232 (5310) (1971) 375–379.
[21] G. Peltzer, F. Crampé, S. Hensley, P. Rosen, Transient strain accumulation and fault interaction in the eastern California shear zone, Geology 29 (11) (2001) 975–978.
[22] A. Hubert-Ferrari, G. King, I. Manighetti, R. Armijo, B. Meyer, P. Tapponnier, Long-term elasticity in the continental lithosphere; modelling the Aden Ridge propagation and the Anatolian extrusion process, Geophys. J. Int. 153 (2003) 111–132.
[23] R.A. Bennett, A.M. Friedrich, K.P. Furlong, Codependent histories of the San Andreas and San Jacinto fault zones from inversion of fault displacement rates, Geology 32 (11) (2004) 961–964, doi:10.1130/G20806.1.
[24] D.P. McKenzie, Plate tectonics of the Mediterranean region, Nature 226 (1970) 239–243.
[25] P. Tapponnier, P. Molnar, Slip-line field theory and large-scale continental tectonics, Nature 264 (1976) 319–324.
[26] J.P. Vilotte, M. Daignières, R. Madariaga, Numerical modeling of intraplate deformation: simple mechanical models of continental collision, J. Geophys. Res. 87 (B13) (1982) 10,709–10,728.
[27] P. England, D.P. McKenzie, A thin viscous sheet model for continental deformation, Geophys. J. R. Astron. Soc. 70 (1982) 295–321.
[28] J. Van der Woerd, P. Tapponnier, F.J. Ryerson, A.-S. Meriaux, B. Meyer, Y. Gaudemer, R.C. Finkel, M.W. Caffee, G. Zhao, Z. Xu, Uniform postglacial slip-rate along the central 600 km of the Kunlun fault (Tibet), from 26Al, 10Be and 14C dating of riser offsets, and climatic origin of the regional morphology, Geophys. J. Int. 148 (2002) 356–388.
[29] J. Van der Woerd, F.J. Ryerson, P. Tapponnier, Y. Gaudemer, R. Finkel, A.S. Meriaux, M. Caffee, G. Zhao, Q. He, Holocene left-slip rate determined by cosmogenic surface dating on the Xidatan segment of the Kunlun fault (Qinghai, China), Geology 26 (8) (1998) 695–698.
[30] H. Li, J. van der Woerd, P. Tapponnier, Y. Klinger, X. Qi, J. Yang, Y. Zhu, Slip rate on the Kunlun Fault at Hongshui Gou, and recurrence time of great events comparable to the 14/11/2001, Mw~7.9 Kokoxili earthquake, Earth Planet. Sci. Lett. 237 (2005) 285–299.
[31] C. Lasserre, P.-H. Morel, Y. Gaudemer, P. Tapponnier, F.J. Ryerson, G.C.P. King, F. Métivier, M. Kasser, M. Kashgarian, B. Liu, T. Lu, D. Yuan, Postglacial left slip rate and past occurrence of M≥8 earthquakes on the western Haiyuan fault, Gansu, China, J. Geophys. Res. 104 (B8) (1999) 17,633–17,651.
[32] R.J. Weldon, K.E. Sieh, Holocene rate of slip and tentative recurrence interval for large earthquakes on the San Andreas fault, Cajon Pass, southern California, Geol. Soc. Amer. Bull. 96 (6) (1985) 793–812.
[33] A. Hubert-Ferrari, R. Armijo, G. King, B. Meyer, A. Barka, Morphology, displacement, and slip rates along the North Anatolian fault, Turkey, J. Geophys. Res. 107 (B10) (2002) 2235, doi:10.1029/2001JB000393.
[34] P. Mann, C.S. Prentice, G. Burr, L.R. Peña, F.W. Taylor, Tectonic geomorphology and paleoseismology of the Septentrional fault system, Dominican Republic, in: J.F. Dolan, P. Mann (Eds.), Active Strike–Slip and Collisional Tectonics of the Northern Caribbean Plate Boundary Zone, Geological Society of America Special Paper, vol. 326, 1998, Boulder, CO.
[35] K. Berryman, Late Quaternary movement on the Wellington Fault in the Upper Hutt area, New Zealand, N.Z. J. Geol. Geophys. 33 (1990) 257–270.
[36] B. Hallet, J. Putkonen, Surface dating of dynamic landforms: young boulders on aging moraines, Science 265 (1994) 937–940.
[37] P. Muzikar, D. Elmore, D.E. Granger, Accelerator mass spectrometry in geologic research, Geol. Soc. Amer. Bull. 115 (6) (2003) 643–654.
[38] F.M. Phillips, J.P. Ayarbe, B.J. Harrison, D. Elmore, Dating rupture events on alluvial fault scarps using cosmogenic nuclides and scarp morphology, Earth Planet. Sci. Lett. 215 (2003) 203–218.
[39] P.L.K. Knuepfer, Changes in Holocene slip rates in strike–slip environments, in: A.J. Crone, E. Omdahl (Eds.), Directions in Paleoseismology, USGS Open-File Report 87-673, 1987, pp. 249–261, Denver.
[40] P.L.K. Knuepfer, Temporal variations in latest Quaternary slip across the Australian–Pacific plate boundary, northeastern South Island, New Zealand, Tectonics 11 (3) (1992) 449–464.
[41] G.J. Lensen, The general case of progressive fault displacement of flights of degradational terraces, N.Z. J. Geol. Geophys. 7 (1964) 864–870.
[42] T.C. Hanks, The age of scarplike landforms from diffusion-equation analysis, in: J.S. Noller, J.M. Sowers, W.R. Lettis (Eds.), Quaternary Geochronology: Methods and Applications, American Geophysical Union, Washington, DC, 2000, pp. 313–338.
[43] G.J. Lensen, Analysis of progressive fault displacement during downcutting at the Branch River terraces, South Island, New Zealand, Geol. Soc. Amer. Bull. 79 (1968) 545–556.
[44] S.M. Bucher, "Strath" as a geomorphic term, Science 75 (1935) (1932) 130–131.
[45] W.B. Bull, Geomorphic Responses to Climatic Change, Oxford University Press, Oxford, 1991, 326 pp.
[46] D.R. Montgomery, Observations on the role of lithology in strath terrace formation and bedrock channel width, Am. J. Sci. 304 (2004) 454–476.
[47] B. Pan, D.A. Burbank, Y. Wang, G. Wu, J. Li, Q. Guan, A 900 k.y. record of strath terrace formation during glacial–interglacial transitions in northwest China, Geology 31 (11) (2003) 957–960.
[48] G.S. Hancock, R.S. Anderson, Numerical modeling of fluvial strath–terrace formation in response to oscillating climate, Geol. Soc. Amer. Bull. 114 (9) (2002) 1131–1142.
[49] B. Poisson, J.P. Avouac, Holocene hydrological changes inferred from alluvial stream entrenchment in north Tian Shan (northwestern China), J. Geol. 112 (2) (2004) 231–249.
[50] R. Hetzel, S. Niedermann, M. Tao, P.W. Kublik, S. Ivy-Ochs, B. Gao, M.R. Strecker, Low slip rates and long-term preservation of geomorphic features in Central Asia, Nature 417 (2002) 428–432.

[51] E.T. Brown, D.L. Bourlés, B.C. Burchfiel, Q. Deng, J. Li, P. Molnar, G.M. Raisbeck, F. Yiou, Estimation of slip rates in the southern Tien Shan using cosmic ray exposure dates of abandoned alluvial fans, Geol. Soc. Amer. Bull. 110 (1998) 377–386.
[52] P. Blisniuk, W.D. Sharp, Rates of late Quaternary normal faulting in central Tibet from U-series dating of pedogenic carbonate in displaced fluvial gravel deposits, Earth Planet. Sci. Lett. 215 (2003) 169–186.
[53] R.P. Suggate, The interpretation of progressive fault displacement of flights of terraces, N. Z. J. Geol. Geophys. 3 (3) (1960) 364–374.
[54] R. Grapes, Comment on "Terrace correlation, dextral displacements, and slip along the Wellington Fault, North Island, New Zealand", N. Z. J. Geol. Geophys. 36 (1993) 131–133.
[55] S. Ouchi, Flume experiments on the horizontal stream offset by strike–slip faults, Earth Surf. Processes Landf. 29 (2004) 161–173.
[56] K.R. Berryman, R.J. Van Dissen, Reply to comment by Grapes on "Terrace correlation, dextral displacements, and slip along the Wellington Fault, North Island, New Zealand", N. Z. J. Geol. Geophys. 36 (1993) 133–135.
[57] G.D. Simpson, J.N. Baldwin, K.I. Kelson, W.R. Lettis, Late Holocene slip rate and earthquake history for the northern Calaveras Fault and Welch Creek, eastern San Francisco bay area, California, Bull. Seismol. Soc. Am. 89 (5) (1999) 1250–1263.
[58] H.A. Cowan, M.S. McGlone, Late Holocene displacements and characteristic earthquakes on the Hope River segment of the Hope Fault, New Zealand, J. R. Soc. N.Z. 21 (4) (1991) 373–384.
[59] K.R. Berryman, Late Quaternary movement on White Creek Fault, South Island, New Zealand, N. Z. J. Geol. Geophys. 23 (1) (1980) 93–101.
[60] J.R. Arrowsmith, D.D. Pollard, D.D. Rhodes, Hillslope development in areas of active tectonics, J. Geophys. Res. 101 (B3) (1996) 6255–6275.
[61] D.B. Nash, Morphologic dating of fluvial terrace scarps and fault scarps near West Yellowstone, Montana, Geol. Soc. Amer. Bull. 95 (1984) 1413–1424.
[62] J.P. Avouac, G. Peltzer, Active tectonics in southern Xinjiang, China: analysis of terrace riser and normal fault scarp degradation along the Hotan–Qira fault system, J. Geophys. Res. 98 (B12) (1993) 21,773–21,807.
[63] J.P. Avouac, P. Tapponnier, M. Bai, H. You, G. Wang, Active thrusting and folding along the northern Tien Shan and Late Cenozoic rotation of the Tarim relative to Dzungaria and Kazakhstan, J. Geophys. Res. 98 (B4) (1993) 6755–6804.
[64] K.L. Pierce, S.M. Colman, Effect of height and orientation (microclimate) on geomorphic degradation rates and processes, late-glacial terrace scarps in central Idaho, Geol. Soc. Amer. Bull. 97 (1986) 869–885.
[65] L. Hsu, J.D. Pelletier, Correlation and dating of Quaternary alluvial-fan surfaces using scarp diffusion, Geomorphology 60 (2004) 319–335.
[66] Z. Washburn, Quaternary tectonics and earthquake geology of the central Altyn Tagh fault, Xinjiang, China: implications for tectonic processes along the northern margin of Tibet, Arizona State University, M.S., 2001.
[67] E. Cowgill, J.R. Arrowsmith, A. Yin, X.-F. Wang, Z. Chen, The Akato Tagh bend along the Altyn Tagh fault, NW Tibet 2: active deformation and the importance of transpression and strain hardening within the Altyn Tagh system, Geol. Soc. Amer. Bull. 116 (11/12) (2004) 1443–1464; doi:10.1130/B25360.1.
[68] R.D. Gold, E. Cowgill, X.-F. Wang, X.-H. Chen, Application of trishear fault-propagation folding to active reverse faults: examples from the Dalong Fault, Gansu Province, NW China, J. Struct. Geol. 28 (2006) 200–219.